N O T I C E

THIS DOCUMENT HAS BEEN REPRODUCED FROM MICROFICHE. ALTHOUGH IT IS RECOGNIZED THAT CERTAIN PORTIONS ARE ILLEGIBLE, IT IS BEING RELEASED IN THE INTEREST OF MAKING AVAILABLE AS MUCH INFORMATION AS POSSIBLE

DOE/NASA/2593-22
NASA TM-81678

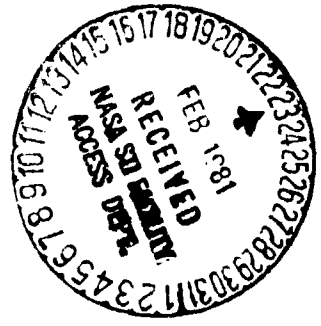

The Effects of Trace Impurities in Coal-Derived Liquid Fuels on Deposition and Accelerated High Temperature Corrosion of Cast Superalloys

Carl E. Lowell, Daniel J. Deadmore,
Gilbert J. Santoro, and Fred J. Kohl
National Aeronautics and Space Administration
Lewis Research Center

Work performed for
U.S. DEPARTMENT OF ENERGY
Fossil Energy
Office of Coal Utilization

Prepared for
Twenty-Sixth Annual International Gas
Turbine Conference sponsored by The American
Society of Mechanical Engineers
Houston, Texas, March 8-12, 1981

DOE/NASA/2593-22
NASA TM-81678

The Effects of Trace Impurities in Coal-Derived Liquid Fuels on Deposition and Accelerated High Temperature Corrosion of Cast Superalloys

Carl E. Lowell, Daniel J. Deadmore,
Gilbert J. Santoro, and Fred J. Kohl
National Aeronautics and Space Administration
Lewis Research Center
Cleveland, Ohio 44135

Work performed for
U.S. DEPARTMENT OF ENERGY
Fossil Energy
Office of zation
Washington, D.C. 20545
Under Interagency Agreement EF-77-A-01-2593

Prepared for
Twenty-Sixth Annual International Gas
Turbine Conference sponsored by The American
Society of Mechanical Engineers
Houston, Texas, March 8-12, 1981

THE EFFECTS OF TRACE IMPURITIES IN COAL-DERIVED LIQUID FUELS ON DEPOSITION AND ACCELERATED HIGH TEMPERATURE CORROSION OF CAST SUPERALLOYS

by

Carl E. Lowell, Daniel J. Deadmore,
Gilbert J. Santoro and Fred J. Kohl
National Aeronautics and Space Administration
Lewis Research Center
Cleveland, Ohio

INTRODUCTION

One of the major materials questions to be raised by the use of coal-derived liquids and gases for powering gas turbines is the question of the effects of the residual impurities on deposition and corrosion. The exact nature and consequences of these impurities and their concentrations is also largely unknown. In an attempt to provide answers to some questions raised by these uncertainties, experimental and analytical studies have been conducted at the Lewis Research Center under support of the Department of Energy's Division of Fossil Fuel Utilization. The general objective of this effort is to help provide a gas turbine technology data base to develop improved gas turbine power conversion systems for coal and coal-derived fuel. Specifically, these studies are aimed at answering some of the questions concerning the effects of fuel impurities on deposition and corrosion of cast superalloys used in the high temperature components of gas turbines.

The studies being conducted contain three major areas:

1. Fuel corrosivity prediction.

   a) Long-time tests of turbine materials in atmospheric pressure combustion rigs burning clean fuels doped with contaminants expected in coal-derived fuels. Development of a life prediction equation (Refs. 1 2 and 3).

   b) Testing of materials in the combustion products of actual coal-derived fuels to verify the life prediction equation developed in part a.

   c) Tests aimed at finding potential fuel additives which would reduce corrosion without extensive fouling (Refs. 4 and 5).

2. Deposition and fouling.

   a) Prediction of deposit composition and dew points based on a thermodynamic treatment and experimental verification of the composition of deposits formed from the combustion of coal-derived fuels (Refs. 6 and 7).

   b) The potential for plugging of advanced airfoil cooling systems operating in the combustion products of coal-derived fuels (Ref. 8).

3. Thermal barrier coatings.

   a) Development of advanced thermal barrier coatings.

   b) Development of advanced bond coats.

This paper summarizes the highlights of the results in the first two areas. More details

are available in the references cited. The results of the third area are reported separately (Ref. 9).

MATERIALS

The compositions of the alloys used in the parametric corrosion and inhibitor tests are given in Table 1. The cobalt-base alloy Mar M-509 is a typical cast vane material which is generally considered to have good hot corrosion resistance due to its high chromium content. The four nickel-base alloys cover a range of hot corrosion resistance. IN-792 and IN-738 are similar in composition and have moderately good hot corrosion resistance. U-700 has somewhat less hot corrosion resistance, while IN-100 has the least resistance to such attack. An iron-base alloy, 304 stainless steel, was included in some of the tests. All of the alloys except the 304 stainless steel were cast by a commercial vendor into the shape shown in Figure 1a. The 304 stainless steel samples were 1.27 cm diameter wrought rods 7.62 cm long. All samples were grit blasted and cleaned with alcohol. Prior to test, each sample was measured along a diameter in the center of the expected hot zone (see Figure 1a) with a bench micrometer to a precision of $\pm$ 2 μm, and weighed to $\pm$ 0.2 mg. The samples used in the hole plugging test were actual airfoils from an aircraft gas turbine engine. For the deposition tests, platinum-rhodium collectors were used -- as will be described below.

PROCEDURES

The burner rig used for all of the tests is basically the one shown in Figure 1b, and has been described in reference 10. Briefly, the rig is a nominal Mach 0.3 type fired with Jet A-1 fuel with a sulfur content of from about 0.02 to 0.05 weight percent. The fuel-to-air mass ratio was varied from about 0.030 to about 0.065. For the parametric corrosion, inhibitor, and hole plugging tests, dopants were added directly into the combustion chamber as aqueous solutions. Except for the deposition test, eight samples were rotated rapidly in front of the exhaust nozzle and reached the desired temperature of from 800 to 1100°C in a few minutes. Most of the tests were cyclic in nature, in which one hour exposure at temperature was followed by a forced-air cooling for three minutes. The cycle was repeated for the duration of the test. Periodically, samples were weighed and replaced. For some of the tests, at intermediate times, samples were removed and others were inserted so that the exposed samples could be examined. When trying to determine the extent of corrosion, samples at the conclusion of the corrosion tests were removed, weighed, washed, and reweighed. Washing consisted of immersion of each sample in 300 cm^3 of water at 80°C, followed by soft brushing in running water, an alcohol rinse, and air drying. These samples were then sectioned along the plane shown in Figure 1a, which is the center of the hot zone where all temperature measurements were made during the run. The cut sections were mounted metallographically, polished, and etched. Measurements were made to determine the maximum penetration and to calculate metal loss. While both the initial and final thicknesses were measured to a precision of $\pm$ 2 μm, experience has shown (Ref. 9) that the resultant value is only accurate at best to $\pm$ 20 μm, and often to $\pm$ 100 μm because of the irregularity of the attack.

The actual fuel tests were run similarly to the corrosion tests, the only difference being that the burner had to be modified in order to burn the two fuel types: SRC-II (solvent refined coal) liquids and a micronized coal-oil mixture. These modifications are described fully in references 6 and 7.

The deposition test procedure is shown schematically in Figure 2. The collector was a platinum-10 weight percent rhodium slightly-tapered hollow cylinder about 1.3 cm long and 1.3 cm in diameter and about 0.13 mm thick. The small size of the collector was chosen to allow uniformity of the temperature over the entire surface of the target. The collector was mounted snugly over a hollow support made of IN-600. The junction of a thermocouple was peened into a hole in the wall of the collector support. The thermocouple leads extended through the support and out of the base. The collector was maintained at a temperature of 900°C for the duration of the deposition test. These runs were continuous, not cyclic. The rate of deposition was determined as the weight of material collected on the target divided by the time of the runs, several hours.

RESULTS AND DISCUSSION

Fuel Corrosivity Prediction

Parametric Corrosion Tests. The data accumulated from these tests are presented in detail in reference 2. The parameters, which were varied in accordance with a statistical design, were the dopant concentrations and the temperature. The dopants were sodium (Na), potassium (K), magnesium (Mg), calcium (Ca), and chlorine (Cl). The concentrations varied from approximately 0.01 wppm to 10 wppm. The ranges are shown schematically in Figure 3. The temperature was varied between 800 and 1100°C. There were 322 points per alloy. The metal recession data from these experiments were fit to a polynomial equation using multi-linear regression. The final model was chosen by a backwards elimination type of regression. It must be pointed out that scaling was required for each variable in order to achieve a reasonable degree of orthogonality among the terms of the model.

Figures 4 through 8 illustrate the effects of the various impurities on corrosive attack and are derived from the model. In Figure 4, we have K at 0.9 ppm, Mg and Ca at 0.1 ppm, Cl at 2.93 ppm, the temperature at 950°C, and the time at 100 hours. Predicted metal recession as a function of Na concentration for each of the four alloys is plotted. Indications of the reliability of the predictive equations are provided by

representative standard error limits on the figures. In Figure 5, a similar plot of metal recession versus Na concentration is presented. However, the Mg and Ca concentrations are increased to 1.0 ppm. A comparison of the two plots shows a general reduction in attack for all alloys with the greater concentrations of Mg and Ca. The reduction is minimal for Mar M-509; it is substantial for IN-100, U-700, and IN-792. Figures 6 and 7 provide similar plots to indicate the effects of Mg and Ca on potassium attack. In general, the same observations can be made: K causes increasing attack with increasing concentration; Mg and Ca tend to reduce such attack. Figure 8 shows the effect of temperature on attack with the other variables held at their nominal center point values, that is, Na and K at 0.9 ppm, Ca and Mg at 0.47 ppm, Cl at 2.93 ppm, and the time at 100 hours. The metal recession of IN-100 decreases with increasing temperature; the metal recession of Mar M-509 increases slightly with increasing temperature; and both IN-792 and U-700 metal recession curves reveal maxima.

Accelerated Corrosion. The impurity elements studied in this series were potassium, vanadium, molybdenum, tungsten, phosphorus. and lead, in combination with sodium. The results were compared with the sodium-only baseline test. It was determined that all of the elements caused corrosion greater than Na alone under some conditions. This work is summarized in Figures 9 through 11. The increased corrosion was indicated by the lowering of the temperature of the onset of hot corrosion. This lowering of the hot corrosion threshold was determined to be due, at least in part, to the formation of low melting point deposits which can flux protective oxide scales (see Table II). The effect of varying the Na/K ratio (Figures 10 and 11) was not large except at concentrations near zero Na, in which case little hot corrosion occurred. However, some hot corrosion did take place when only K was present even though the test was conducted at a metal temperature more than 150°C below the melting point of the potassium sulfate deposit.

Actual Fuel Tests

Two types of fuels were utilized in these tests. One was the SRC-II naphtha fuel, while the second was a micronized coal-oil mixture. The compositions of these fuels are shown in Tables III and IV. For both fuel types, extensive modifications had to be made to the burner rig in order to get them to burn consistently. These extensive modifications are detailed in references 6 and 7. Because of the difficulty of burning these fuels, even after the modifications, the test of the SRC-II naphtha was limited to approximately 190 hours while the test of the micronized coal-oil mixture was limited to about 45 hours. In both cases, the Na and K levels in the fuel were low enough as to lead one to predict essentially no hot corrosion attack based on the work described above. This was, indeed, the case as is shown in Figures 12 and 13. The microstructures confirm that the corrosion attack is the same as that found in oxidation tests, but do show extensive deposits formed on the surfaces of the samples. Thus, the conclusion drawn from this work is that while no potential for hot corrosion is likely to exist, deposition and fouling is likely to be a problem when using these fuels.

Inhibition

In this series of tests, a number of additives were used in an attempt to find an effective inhibitor for hot corrosion. The elements considered were aluminum (Al), silicon (Si), iron (Fe), chromium (Cr), zinc (Zn), magnesium (Mg), calcium (Ca), and barium (Ba). While all of these additives reduced hot corrosion for some alloys, the most effective and consistent additive was Ba. For all alloys (see Figure 14), this Ba addition reduced the corrosion attack to nearly oxidative attack levels. Later work indicated that strontium (Sr) was equally effective. As can be seen in Figure 15, the microstructure of alloys protected by Ba inhibition show an extensive barium sulfate coating on the outer surface of the alloy. This coating is quite dense and accounts for the major part of the inhibiting effect of the Ba. Unfortunately, this can lead to fouling.

In an attempt to reduce fouling while retaining the beneficial effects of the alkaline earth inhibitors on hot corrosion of superalloys, both the use of additives and pretreatments with Ba and/or Sr were evaluated. Si, as an additive with the Ba inhibitor, showed some promise (see Table V). Total deposition was apparently reduced while the inhibition of hot corrosion by Ba was unimpaired. Pretreatment with the inhibitor (see Figure 16) was found to be much more effective and controllable. From a comparison of the two techniques, some conclusions were drawn. None of the secondary additives produced dramatic decreases in fouling, and indeed there is some evidence that even under ideal situations some loss in inhibition was apparent. The pretreatment of the inhibitors, however, was shown to have definite potential; such a technique can be used to keep fouling under close control. The specific parameters for intermittent application and the effectiveness of this approach will be related to such factors as the specific turbine operating conditions, the impurities in the fuel, etc. It does, however, offer a flexible way to meet changing Na and K levels found in the combustion gases of turbines burning coal-derived or heavy-distillate petroleum fuels or ingesting airborne salt.

Deposition

Thermodynamic Prediction of Deposition. Four cuts of SRC-II fuels were used in this test. One was a naphtha, the second a light oil, the third a wash solvent, and finally a mid:heavy distillate blend. The analyses of these fuels are shown in Table III. The major metallic elements which contributed to the deposits were copper, iron, chromium, calcium, aluminum, nickel, silicon, titanium, zinc, and sodium. The deposits were found to be mainly metal oxides (see Table VI). An equilibrium

thermodynamic analysis was employed to predict the chemical composition of the deposits. Agreement (See Table VI) between the predicted and observed compounds was excellent. As a result, considerable confidence in the ability to determine deposit composition from thermodynamic considerations was gathered.

Hole Plugging. A summary of the hole-plugging tests, conditions, and results is given in Table VII. Three tests were made with dopant A and four with dopant B as defined in Table VII. The metal temperature at the start of the test was 815°C in all cases, and 815 ± a T at the conclusion of the test. Flame temperature and cooling air mass flow were the major variables. However, they were not independent of each other at the higher flame temperatures required to bring the initial leading edge temperatures to 815°C. Figure 17A is a photograph of a post-test blade which had very little leading edge temperature rise (11°C); a value close to the sensitivity of the temperature measurement. The holes show very little evidence of plugging, although there is a measurable deposit along the leading edge. The coolant-to-hot gas mass flow ratio of 2.3 is quite high. In contrast, a second blade (Figure 17B), which had a measurable leading edge increase of 30°C, shows a complete closure of the holes. The coolant-to-hot gas mass flow ratio of 0.4 for the latter is low for leading edge film cooling holes. These results are similar to the results of vane testing determined in reference 11.

In general, the amount of cooling hole plugging caused by dopant B (Table VII), as determined by metal temperature rise, was greater for similar test conditions than dopant A. This confirms the earlier conclusions of the work in reference 10 that phosphorous (P), in combination with Fe and Ca, greatly accelerates the tendency for hole plugging. The effect of cooling air flow on hole plugging is shown graphically in Figure 18. In general, at low or no air cooling flow, any deposit will plug the holes. As the cooling flow rate increases, the tendency for plugging is reduced markedly, and above a certain value no plugging is observed at all. The amount of flow required to keep the holes open is a strong function of the impurity content of the fuel. It appears probable that any composition could be prevented from depositing by sufficient cooling mass flow. Whether an engine designer could afford to divert sufficient air flow to keep the holes clear and still retain sufficient cycle efficiency would depend strongly on the nature of the deposit, the cycle efficiency and penalty associated with increased cooling air requirements.

SUMMARY OF RESULTS

The prime results of the studies reported herein may be briefly summarized as follow:

1. An empirical model has been developed to allow the estimation of hot corrosion attack of several cast superalloys over a range of sodium, potassium, calcium, magnesium, and chlorine fuel impurity contents and over the temperature range of 800 to 1000°C for times to 1000 hours.

2. The potential effects of vanadium, molybdenum, tungsten, phosphorus, and lead impurities, in combination with sodium, on accelerated corrosion have been estimated: all of these elements caused corrosion at greater rates than sodium alone, under the same test conditions.

3. Inhibition of hot corrosion can be effectively accomplished by the use of strontium and barium, at least to temperatures of 900°C.

4. The fouling caused by the use of such inhibitors can be markedly reduced by pretreatment while still retaining their beneficial aspects.

5. Thermodynamic equilibrium calculations can be used to effectively calculate the composition of deposits formed as a result of the combustion of coal-derived liquids.

6. The potential for hole plugging is present during the combustion of these coal-derived liquids; however, its extent is greatly dependent upon the exact nature of the impurities in the synthetic fuels. This potential, however, is heightened in cooling schemes where cooling velocities are at a minimum.

REFERENCES

1. Lowell, C. E., Sidik, S. M., and Deadmore, D. L., "Effect of Sodium Potassium, Magnesium, Calcium, and Chlorine on the High Temperature Corrosion of IN-100, U-700, IN-792, and Mar M-509," ASME Paper 80-GT-150, 1980.

2. Lowell, C. E., Sidik, S. M., and Deadmore, D. L., "High Temperature Alkali Corrosion in High Velocity Gases," in preparation.

3. Deadmore, D. L. and Lowell, C. E., "Effects of Impurities in Coal-Derived Liquids on Accelerated Hot Corrosion of Superalloys," NASA TM-81384, 1980.

4. Deadmore, D. L. and Lowell, C. E., "Inhibition of Hot Salt Corrosion by Metallic Additives," NASA TM-78966, 1978.

5. Deadmore, D. L. and Lowell, C. E., "Fouling and the Inhibition of Salt Corrosion," NASA TM-81469, 1980.

6. Santoro, G. J., et al., "Deposition and Material Response from Mach 0.3 Burner Rig Combustion of SRC-II Fuels," NASA TM-81634, 1980.

7. Santoro, G. J., Calfo, F. D., and Kohl, F. J., "Material Response from Mach 0.3 Burner Rig Combustion of a Coal-Oil Mixture," NASA TM, in preparation.

8. Deadmore, D. L. and Lowell, C. E., "Airfoil Cooling Hole Plugging by Combustion Gas Impurities of the Type Found in Coal-Derived Liquids," NASA TM-79076, 1979.

9. Hodge, P. E., et al., "Review of NASA Progress in Thermal Barriers for Stationary Gas Turbines," NASA TM, in preparation.

10. Lowell, C. E. and Deadmore, D. L., "Effect of a Chromium-Containing Fuel Additive on Hot Corrosion," Corrosion Science, Vol. 18, 1978, pp. 747-763.

11. Deadmore, D. L. and Lowell, C. E., "Plugging of Cooling Holes in Film-Cooled Turbine Vanes," NASA TM X-73661, 1977.

TABLE I. - COMPOSITION OF CAST SUPERALLOYS TESTED

(All values are weight percent)

Element	Mar M-509	IN-792	IN-738	U-700	IN-100	304 SS
Cr	23	12.7	16	14.2	10	19
Ni	10	Bal.	Bal.	Bal.	Bal.	10
Co	Bal.	9.0	8.5	15.5	15	---
Al	---	3.2	3.4	4.2	5.5	---
Ti	.2	4.2	3.4	3.3	4.7	---
Mo	---	2.0	1.8	4.4	3.0	---
W	7	3.9	3.9	---	---	---
Ta	3.5	3.9	.9	---	---	---
Nb	---	.9	---	---	---	---
V	---	---	---	---	1.0	---
Mn	---	---	.2	<.01	---	2.0
Fe	---	---	.5	.1	---	Bal.
Si	---	---	.3	<.1	---	1.0
Zr	.5	.1	.1	<.01	.06	---
B	---	.02	.01	.02	.014	---
C	.6	.2	.17	.06	.18	.08

TABLE II. - PHASES DEPOSITED FROM DOPED FUEL COMBUSTION

Dopants (wppm)	X-ray diffraction identification of deposited phases	Melting point, °C
3Na	Na_2SO_4 (Forms I, III, and V)	884
3V	$NiO.V_2O_5$	~710
3Na+3V	Na_2SO_4 (V, III)	884
	$\alpha NaVO_3$	630
	VO_2	---
3Na+3Mo	Na_2SO_4 (V, III)	884
	$Na_2Mo_2O_7$ [a]	612
3Na+3W	Na_2SO_4 (V)	884
	Na_2WO_4 [a]	698
3Na+12W	Na_2WO_4,	698
3Na+3P	Na_3PO_4	---
	Glass	---
3Na+3Pb	$PbSO_4$	1077[b]
	Na_2SO_4 (V, III)	884
2.25Na+0.75K	Na_2SO_4 (III)	884
	$Na_xK_{2-x}SO_4$	~825[c]
1.5Na+1.5K	$Na_xK_{2-x}SO_4$	~870
0.75Na+2.25K	$Na_xK_{2-x}SO_4$	~950
3K	K_2SO_4	1071

[a]Some hydrate formed on cooling.
[b]Eutectic at 730°C.
[c]Solidus.

Table III. - COMPOSITION AND PROPERTIES OF SRC-II FUELS. Trace elements analysis for the naphtha reported in this Table was for a sample of fuel taken at a point in time when the deposition/corrosion test had been run for 191 one-hour cycles. Trace element values marked with an "*" are considered in the thermodynamic prediction of deposition.

	SRC-II fuel type			
Major elements (weight percent)	Naphtha	Light oil	Wash solvent	Mid: heavy distillate blend
Carbon	84.61 (84.62)[a]	80.45	84.12	86.21
Hydrogen	11.64 (12.09)	9.75	8.80	8.64
Oxygen	3.16 (2.33)	9.17	6.34	3.99
Nitrogen	9.61 (0.58)	0.42	0.53	0.95
Sulfur	0.61 (0.38)	0.40	0.33	0.27
Ash	N.D.[b]	N.D.	N.D.	0.02
Trace elements (wppm)				
Al	<0.01	<0.01	0.9*	1.0*
B	0.08	<0.06	<0.06	<0.09
Ca	<0 01	0.1*	0.6*	0.3*
Cl	49.*	<10	<10	294.*
Cr	0.1*	0.04	0.06	1.8*
Cu	28.9*	0.03	<<0.01	<0.1
Fe	8.8*	158.*	35.7*	7.0*
K	<0.25	0.2*	0.4*	<0.1
Mg	<<0.01	0.08	0.07	0.08
Mn	0.05	0.4	0.3	0.2
Mo	<<0.01	<0.01	<0.01	<<0.01
Na	<0.25	0.6*	0.3*	0.5*
Ni	4.8*	0.1*	<<0.01	0.1*
P	<5	<6	<6	<7
Pb	0.3*	<0.07	<0.06	<0.04
Si	0.09	<0.03	0.5*	1.1*
Sn	0.2	<0.06	<0.06	<0.07
Ti	0.03	<0.01	0.8*	0.2*
V	<<0.01	<0.01	<0.2	0.07
Zn	10.5*	2.5*	0.8*	0.1*
Zr	<<0.01	<0.01	<0.02	<0.02
Heat of combustion, lower heating value (Btu/lb)	18,497	16,551	16,748	17,590
Chemical composition (vol. percent)				
Aromatics	33.0	43.6	62.0	-
Olefins	6.0	-	-	-
Saturates	61.0	-	-	-
Sp. Gravity 60/60°F	0.824	-	-	0.999
Viscosity, 100°F, cSt	0.816	-	-	4.527

[a] Values in parentheses are analyses provided by the supplier upon shipment of SRC-II naphtha.

[b] N.D. = not determined.

Table IV. - COMPOSITION AND PROPERTIES OF COAL-OIL-MIXTURE FUEL (40 WEIGHT PERCENT PITTSBURGH-SEAM COAL IN NO. 2 FUEL OIL)

Elemental composition (weight percent)			
C	82.5	Al	0.65
H	9.5	Ca	0.14
N	0.6	Fe	0.35
O	2.8	K	0.028
S	0.32	Mg	0.024
Cl	0.047	Na	0.012
Ash	3.7	Si	1.9
		Ti	0.042
Trace metals (wppm)			
Co	5		
Cr	25		
Cu	12		
Mn	40		
Ni	35		
Sr	20		
V	10		
Zr	15		
Heat of combustion, higher heating value (Btu/lb)		17,020	
Density (g cm^{-3})		1.06	
Viscosity, 70°f (centipose)		4000±1000	

TABLE V. - DEPOSITION AND METAL RECESSION WITH ADDITIONS TO BARIUM INHIBITED HOT CORROSION

Additives	Metal recession (μm)				Deposit after washing (g)			
(wppm)	IN-100	U-700	IN-792	Mar M-509	IN-100	U-700	IN-792	Mar M-509
3Na+3Ba+3Ca	410	74	61	70	-0.99[a]	0.86	0.88	0.93
3Na+3Ba+3Mg	1680	62	100	80	-7.19[a]	.52	.61	.58
3Na+3Ba+3Sr	23	47	10	61	1.00	.78	.92	.97
3Na+3Ba+3Si	58	29	40	60	.04	.32	.29	.55
3Na+3Ba+3Al	705	58	43	59	-1.00[a]	.32	.32	.32
3Na+3Ba+3B	401	70	123	78	-1.60[a]	.38	.57	.64
3Na+3Ba+3Mn	1587	60	86	44	-6.53[a]	.32	.32	.40
3Na+3Ba+3Ni	819	52	83	42	-5.08[a]	.51	.63	.60
3Na+3Ba+3Zn	598	38	36	56	-3.04[a]	.35	.43	.42
3Na+3Ba+3P	1439	285	244	172	-3.82[a]	-.55[a]	.07	.04
3Na+3Ba+3Pb	1209	66	66	59	-4.69[a]	.57	.57	.57
3Na	2158	453	760	231	---	---	---	---
3Na+1Ba	48	54	44	44	.03	.88	.81	.64

[a]Net loss, i.e., corrosion excessive.

Table VI. - DEPOSITION AND MATERIAL RESPONSE FROM MACH 0.3 BURNER RIG COMBUSTION OF SRC-II FUELS

Comparison of Predicted and Actual Deposit Compositions

	Fuel type (all solvent refined coal liquids (SRC-II)			
	Naphtha	Light oil	Wash solvent	Mid: heavy distillate blend
Major deposit phases predicted to form (Based on trace element chemical analysis of fuel)	Cu_2O(s)[a] CuO(s) $NiFe_2O_4$(m) Fe_2O_3(m)	Fe_2O_3(s)	Fe_2O_3(s)	Fe_2O_3(s) Cr_2O_3(m)
Actual deposit collected (identified by x-ray diffraction)	CuO(s) $(Cu,Ni,Zn)Fe_2O_4$(s) $(Cu_{0.2}Ni_{0.8})O$(m)	Fe_2O_3(s)	Fe_2O_3(s) Fe_3O_4(s)	Fe_2O_3(s)

[a] s = strong; m = medium

TABLE VII. - HOLE PLUGGING CONDITIONS AND RESULTS

A. Dopant compositions in ppm by weight of combustion products

Element	Dopant A	Dopant B
Fe	2.0	2.0
Pb	.05	.05
Ca	.1	.1
Na	.5	.5
K	.1	.1
P	---	.5

B. Run summary

Number	Flame temperature[a] (°C)(°F)	Dopant	$\frac{(\rho V)_C}{(\rho V)_H}$ [b]	Leading edge ΔT (°C)	$\frac{\text{Total cooling flow}}{\text{flame temperature}}$
SH-1	1300 (2374)	A	1.0	72*10	11×10^{-5}
SH-2	1550 (2822)	A	2.3	11	27
SH-3	1800 (3272)	A	3.8	28	40
SH-3A	1100 (2012)	B	.4	39	4
SH-1A	1220 (2228)	B	.9	89	9
SH-4	1300 (2374)	B	1.0	111	11
SH-5	1550 (2822)	B	2.3	56	24

[a] Measured with a sonic velocity thermocouple probe.
[b] ρ = density, V = velocity, C = cooling air, and H = combustion gases.

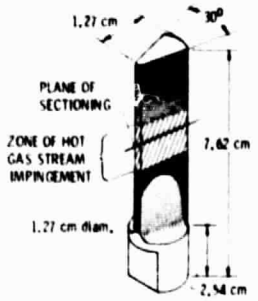

(a) TEST BAR.

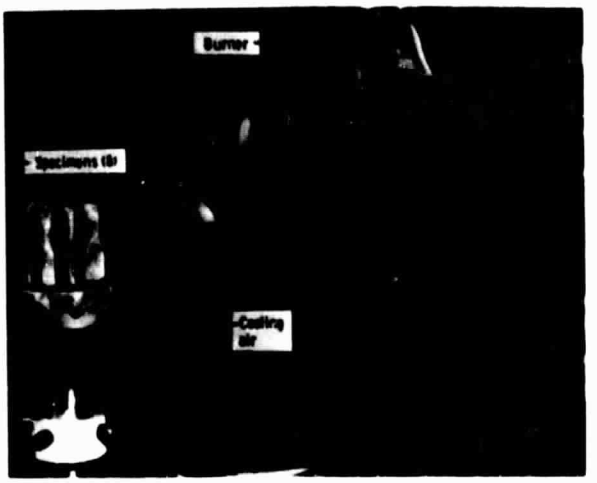

Fig. 1 Hot corrosion apparatus and test specimen.

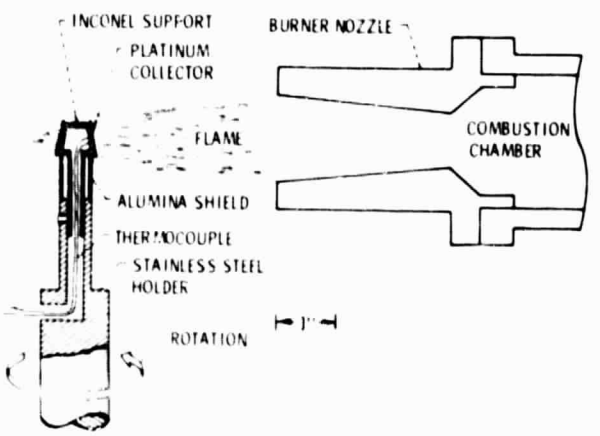

Fig. 2 Schematic of burner-rig salt deposition apparatus.

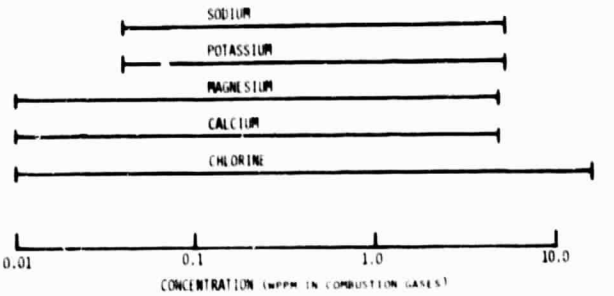

Fig. 3 Impurity ranges in doped fuel experiments.

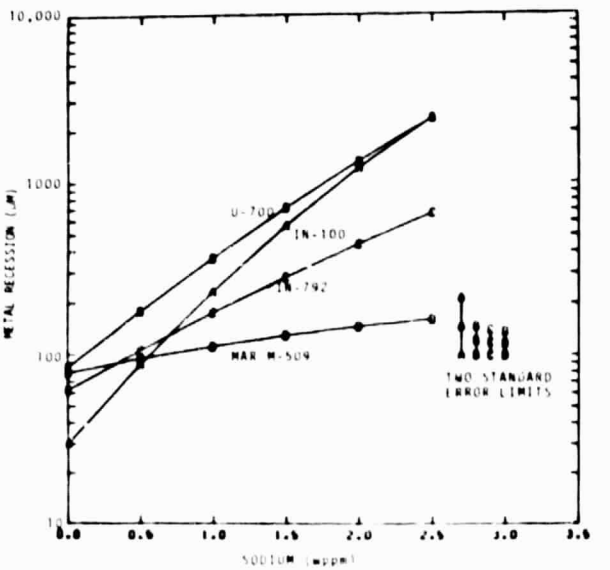

Fig. 4 Hot corrosion attack as a function of sodium concentration: potassium = 0.9 wppm, magnesium and calcium = 0.10 wppm, chlorine = 2.93 wppm, T = 950°C, and time = 100 hours.

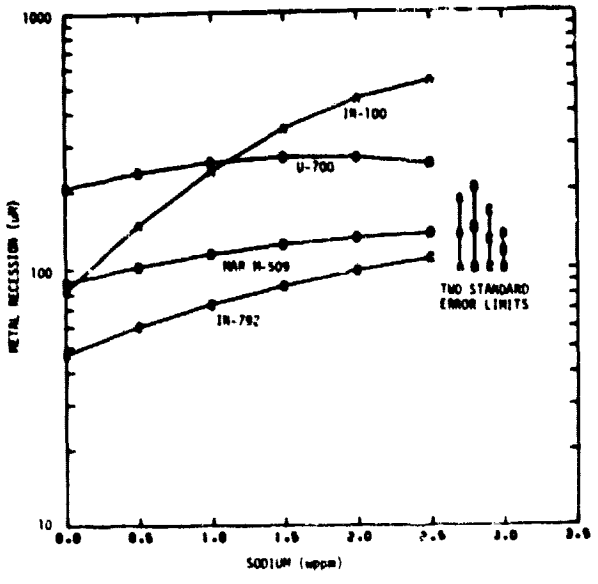

Fig. 5 Hot corrosion attack as a function of sodium concentration: conditions the same as for Fig. 4, except magnesium and calcium = 1.0 wppm.

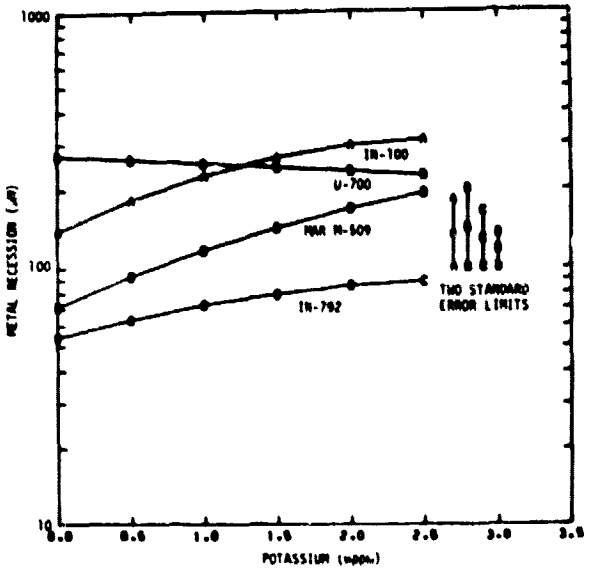

Fig. 7 Hot corrosion attack as a function of potassium concentration: conditions the same as for Fig. 6, except that magnesium and calcium = 1.0 wppm.

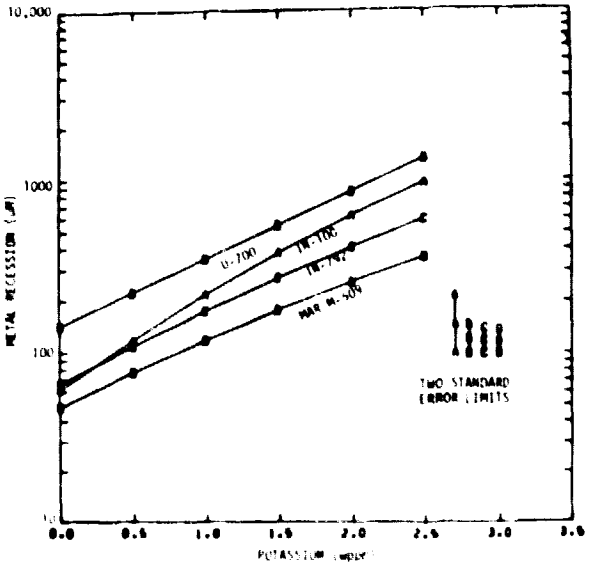

Fig. 6 Hot corrosion attack as a function of potassium concentration: sodium = 0.9 wppm, magnesium and calcium = 0.1 wppm, chlorine = 2.93 wppm, T = 950°C, and time = 100 hours.

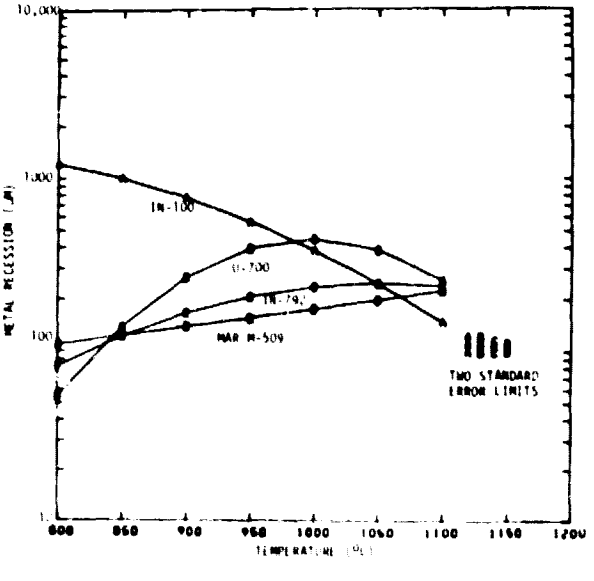

Fig. 8 Hot corrosion attack as a function of temperature: sodium and potassium = 0.9 wppm, magnesium and calcium = 0.47 wppm, and time = 100 hours.

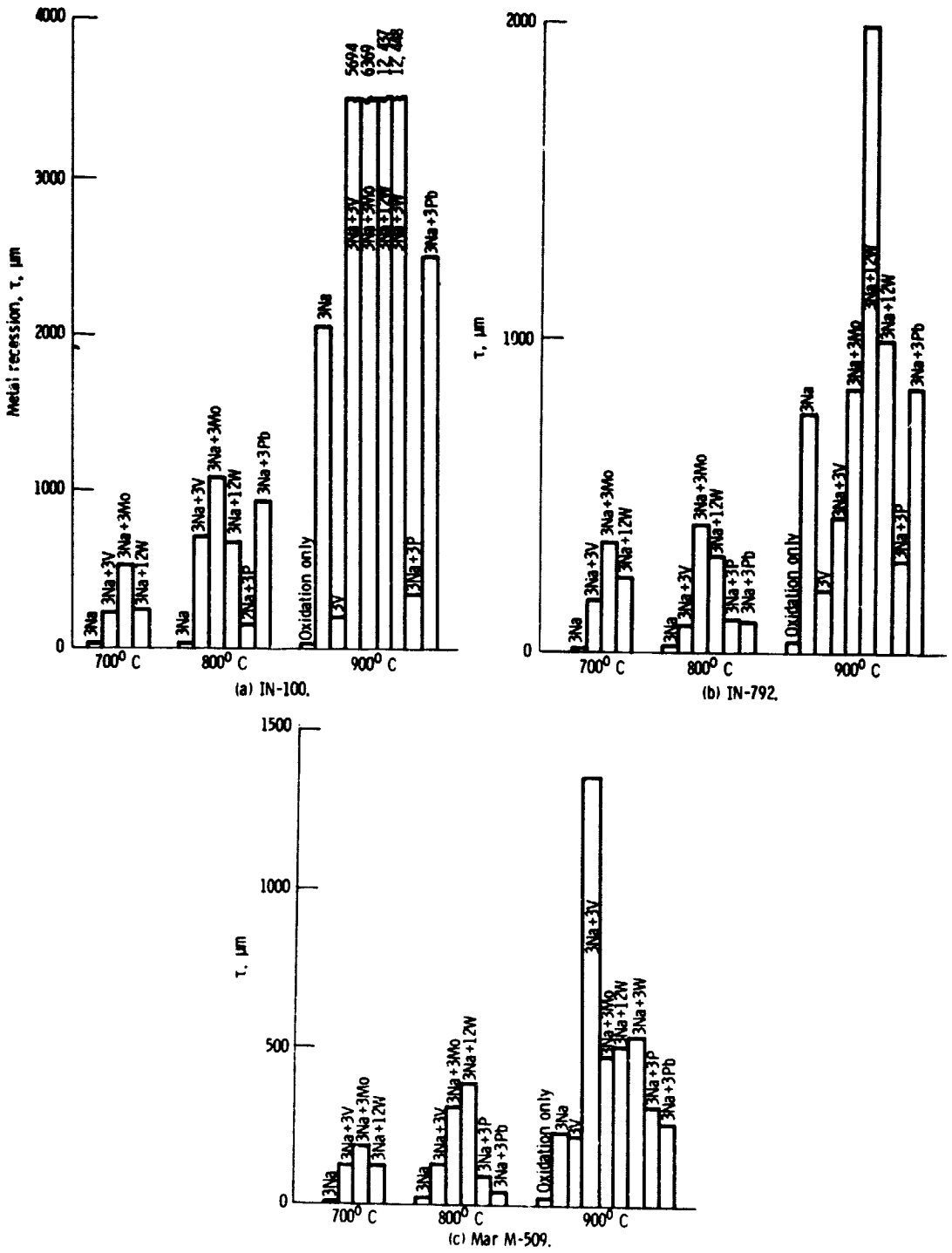

Fig. 9 Effort of potential coal-derived liquid fuel impurities on hot corrosion. One hundred cycles of 1 hour at temperature in a Mach 0.3 burner rig.

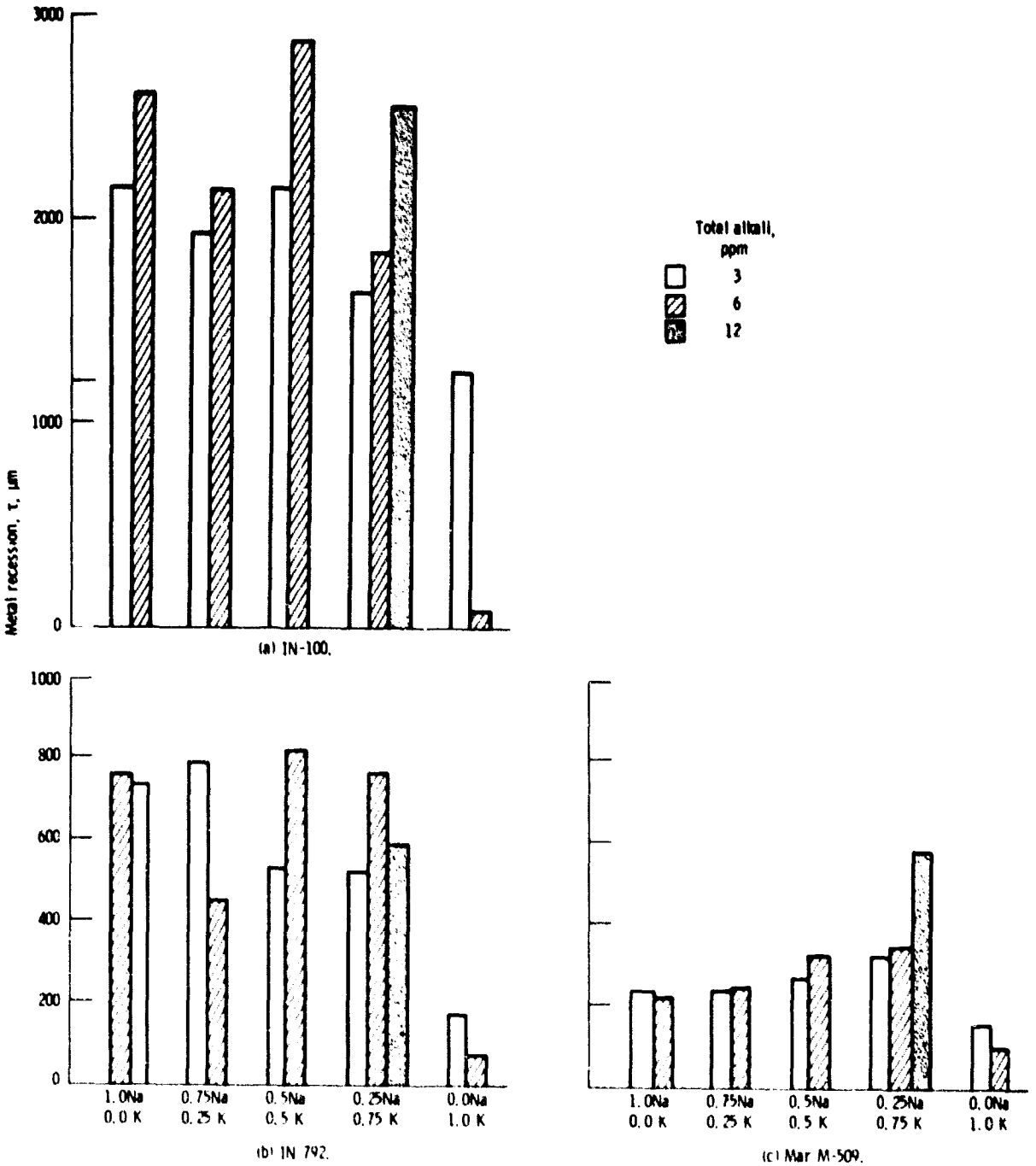

Fig. 10 Effect of Na/K ratio on hot corrosion. One hundred cycles of 1 hour at 900°C in a Mach 0.3 burner rig.

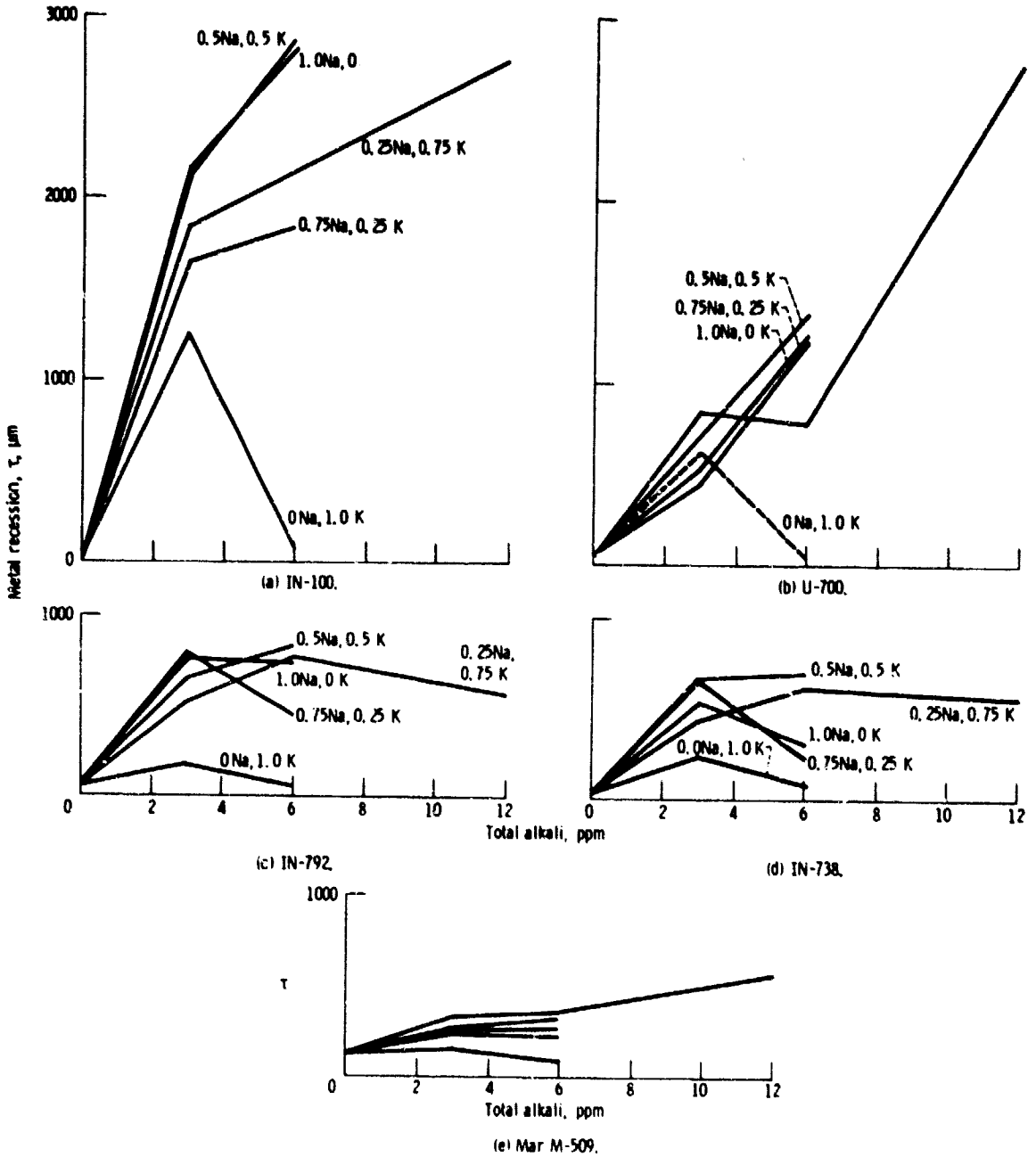

Fig. 11 Effect of total alkali on hot corrosion. One hundred cycles of 1 hour at 900°C in a Mach 0.3 burner rig.

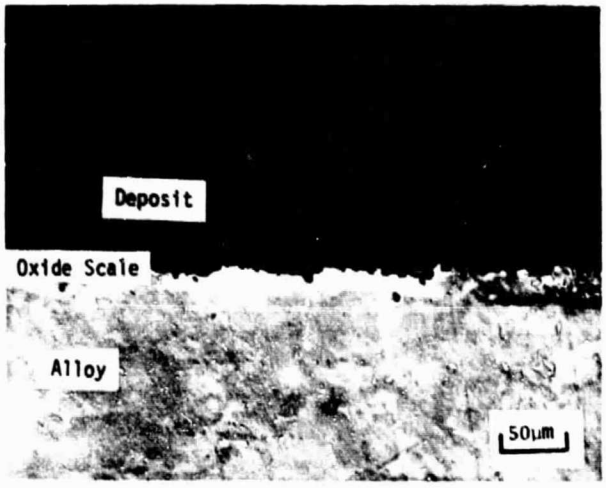

Fig. 12 Deposit morphology on IN-100 exposed in a Mach 0.3 burner rig fueled with SRC-II naphtha.

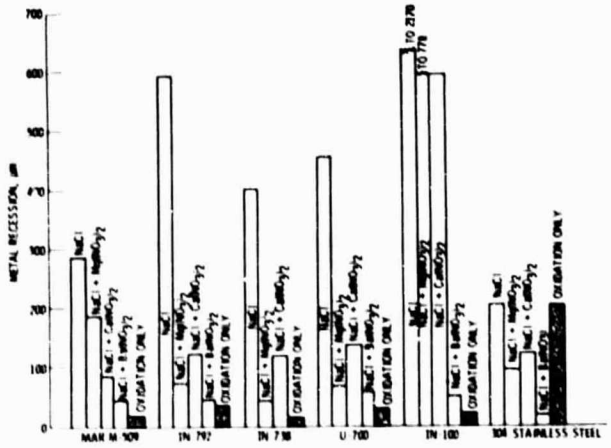

Fig. 14 Effect of alkaline earth additions on burner rig hot corrosion after 100 1-hour cycles at 900°C. All additive concentrations are at 3 ppm of each metal.

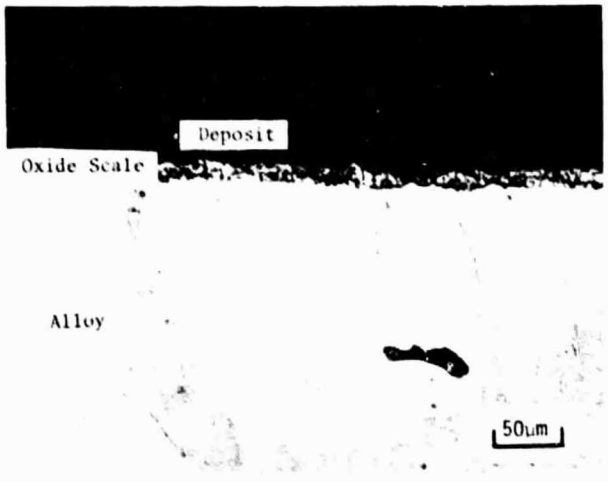

Fig. 13 Deposit morphology on IN-100 exposed in a Mach 0.3 burner rig fueled with a coal-oil mixture.

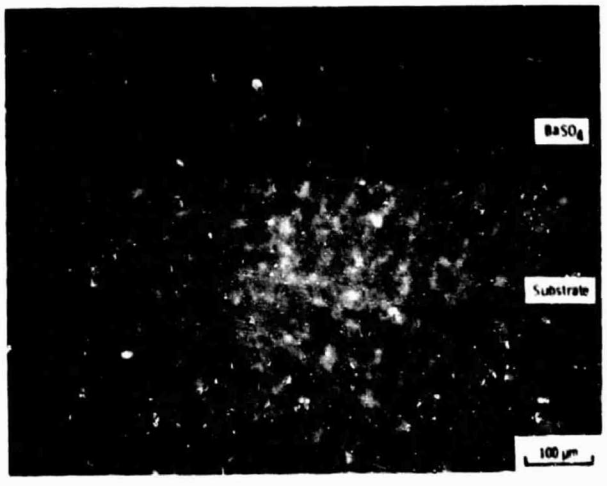

Fig. 15 Deposit of $BaSO_4$ on IN-792 after 100 1-hour cycles at 900°C in the Mach 0.3 burner rig with 3 ppm Ba + 3 ppm Na as NaCl.

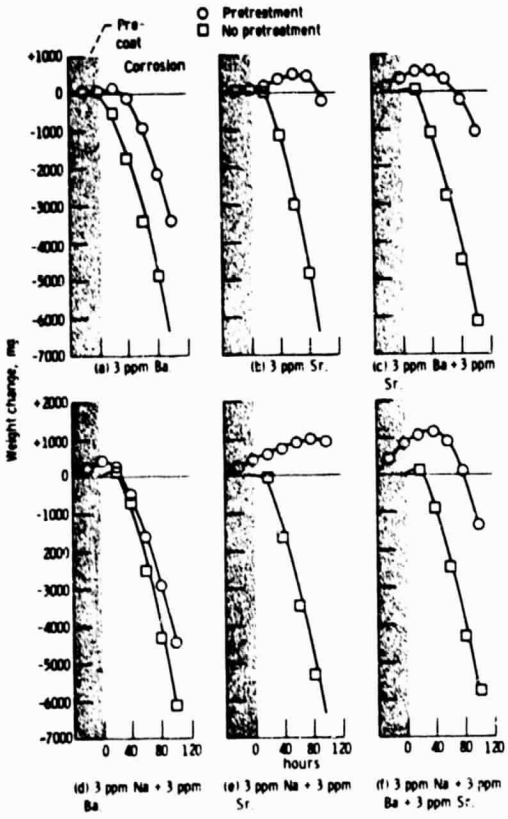

Fig. 16 Effect of various pretreatments of alkaline earths for 40 hours on the hot corrosion of IN-100 with 3 ppm Na as NaCl in the Mach 0.3 burner rig at 900°C.

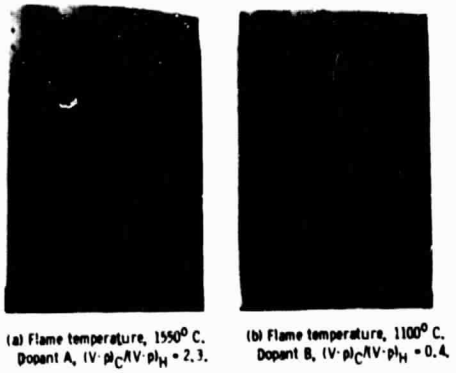

(a) Flame temperature, 1550° C. Dopant A, $(V \cdot p)_C/(V \cdot p)_H = 2.3$.

(b) Flame temperature, 1100° C. Dopant B, $(V \cdot p)_C/(V \cdot p)_H = 0.4$.

Fig. 17 Mass flow-temperature efforts on cooling hole plugging.

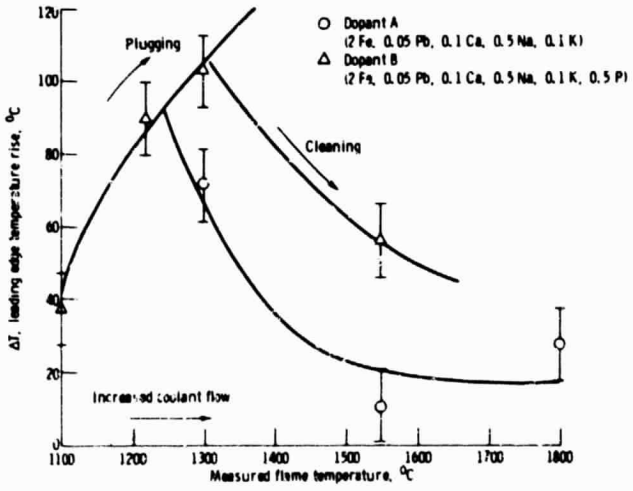

Fig. 18 Large cooling flows required to maintain leading edge temperature at 815°C reduce cooling hole plugging.